



**AIAA-2005-2383**

**Orbital Debris Shape and Orientation Effects on Ballistic Limits**

S. Evans

NASA-Marshall Space Flight Center

Huntsville, AL

and

J. Williamsen

Institute for Defense Analyses

Alexandria, VA

**46<sup>th</sup> Structures, Structural Dynamics, and Materials  
Conference  
18-21 April, 2005  
Austin, TX**

For permission to copy or republish, contact the copyright owner named on the first page.

For AIAA-held copyright, write to AIAA Permissions Department,

1801 Alexander Bell Drive, Suite 500, Reston, VA, 20191-4344.

## Orbital Debris Shape and Orientation Effects on Ballistic Limits

Authors:	Dr. Steven W. Evans Mail Stop EM50 Space Environmental Effects Branch NASA-Marshall Space Flight Center Huntsville, AL Phone: (256) 544-8072 Email: steven.w.evans@nasa.gov	Dr. Joel Williamsen Space and Air Vehicle Vulnerability Operational Evaluation Division Institute for Defense Analyses Alexandria, VA Phone: (703) 578-2705 E-mail: jwilliam@ida.org
----------	---	--

### Abstract

The SPHC hydrodynamic code was used to evaluate the effects of orbital debris particle shape and orientation on penetration of a typical spacecraft dual-wall shield. Impacts were simulated at near-normal obliquity at 12 km/sec. Debris cloud characteristics and damage potential are compared with those from impacts by spherical projectiles. Results of these simulations indicate the uncertainties in the predicted ballistic limits due to modeling uncertainty and to uncertainty in the impactor orientation.

In support of the Columbia Accident Investigation Board (CAIB), the NASA Johnson Space Center (JSC) Safety and Mission Assurance (S&MA) Directorate contracted with the Institute for Defense Analyses (IDA) to conduct a systematic review of potential causes of failure, including impacts by meteoroids or orbital debris (M/OD) (Ref. 1). One of the central findings in the IDA review was that NASA's critical M/OD risk predictions contain a number of significant input uncertainties. One of the largest of these uncertainties appears due to the lack of non-spherical shape considerations in NASA's orbital debris environment and penetration models. As a first step in correcting this lapse, the report suggested that NASA perform a sensitivity analysis for the expected range of effects on damage considering spherical vs. non-spherical impactors.

The latest version of the NASA orbital debris model is ORDEM2000, which was released for use in May 2002. This model utilizes updated in-situ impact data and ground-based radar data to form an empirical model of the current orbital debris flux, with predictions for flux growth in the out-years based on the NASA EVOLVE model. The Satellite Breakup Model (SBM) is the component of EVOLVE that derives an area-to-size relationship for small orbital debris particles (Ref. 2) based on radar cross section (RCS) measurements from the Haystack and Goldstone stations. The debris particle "size" distribution is stated in terms of characteristic length,  $L_c$ . The SBM area-to-size relationship assumes that particles with  $L_c$  below 1.66 mm are cubes, whereas particles above this size become increasingly "potato chip-" or "flake-" shaped, e.g., a particle with an  $L_c$  of 5.3 mm has a length-to-thickness ratio of 3. These shapes are consistent with the RCS-to-size conversion from the Haystack radar data and the mass-to-size relationships from the Spacecraft Orbital Debris Characterization Impact Test (SOCIT) fragment measurements (though not all SOCIT fragments had this type of shape).

In order to examine the sensitivity of impact damage to both the shape of an orbital debris particle and its orientation at impact, we made use of the SPHC hydrodynamic code. This code implements the smooth particle hydrodynamics method in simulating impacts, and was previously compared to other codes and to the predictions of several familiar penetration equations (Ref. 3). For this study the code was run on Pentium IV™ desktop computers under the Windows 2000™ operating system. The runs were fully three-dimensional simulations, reserving memory for up to 210,000 SPH particles. The projectiles and bumper layer were 2024 aluminum, and the backwall was 2219. The Whipple shield configuration was a 1.6-mm bumper, 12-cm standoff, and a 3.2-mm backwall, the same as that used in Ref. 3.

We created an algorithm to assign length and thickness proportions to our impactors, based on data from SBM, for input values of  $L_c$ . We selected five impactor orientations to examine the effect of this parameter on the resulting debris clouds and damage to the backwalls. Sketches of our impact orientations are shown in Figure 1. The impact speed in all simulations was 12 km/s, and the velocity obliquity was 1.6 deg off the normal – this was done in order to break any gridding symmetries.

Figure 2 shows the simulation setups for a sphere and a flake, both with  $L_c = 0.6$  cm. The sphere's mass was 0.314 g, and the flake's was 0.115 g. The flake setup corresponds to the "Face A-B (45-45)" example in Figure 1. Figure 3 compares the debris clouds of these simulations at 8 microseconds into the events. The flake's debris cloud lacks the low-density lead element of the sphere's, and has a concentration of dense material in an arc at approximately the vertical location of the sphere's central fragment mass. This arc is aligned along what were the normals to the flake's largest (square) faces. Nestled in the center of the arc is a barely-fractured remnant of the trailing corner of the flake. The development of this arc structure along the flake face normals is seen in debris clouds from other orientations as well. Figure 4 compares the backwall damage due to these projectiles at the 100 microsecond point. While both projectiles fail the backwall, the damage characteristics are distinctly different. The sphere produces a collection of small perforations near the center of the backwall, several of whose margins have coalesced to make what should develop into a set of jagged petals at later times. The flake produces a lenticular rip in the backwall, aligned with the dense debris arc and flake face normal line. Such a linear hole might cause the backwall to be more subject to an "unzipping" failure at later times if it happened to fall near the wall's principle stress axis. At this stage the flake's hole size is several times that of the sphere's for this orientation, but whether this difference is maintained at later times is unknown.

Hu and Schonberg (Ref. 4) reported that non-spherical impactors were much more damaging than spherical impactors of the same mass. We concur in this finding, since the case above shows that a square flake can produce greater damage than a spherical impactor of over 2.5 times the mass. However, the quantity observed in the debris population is not mass, but RCS, which is directly related to  $L_c$ . We prefer to develop ballistic limits based on this observed variable, but owing to the constraints of time, we can only report results obtained at 12 km/s, comparing flakes to spheres.

Accordingly, we varied  $L_c$  for each of the five orientations shown in Figure 1, and recorded the  $L_c$  values for which the projectile produced four classes of backwall damage: clearly visible through-holes; spallation of SPH particles with accompanying backwall fracture, but no discernable through-holes; fractured back surface particles, but no spallation; and plastic deformation without fracture of the back surface. The  $L_c$  values, corresponding masses, and resulting damage are shown in Table 1. The  $L_c$  values in this table define a ballistic limit band applicable to these non-spherical particles at an impact speed of 12 km/s. The smallest values of  $L_c$  resulting in clearly visible perforations define an upper bound to this band, each applicable to its specific orientation. The largest values of  $L_c$  resulting in plastic-deformation-only define the lower bound of the band, again for each specific orientation. For each orientation the shift from fracture-only to production of through-holes constitutes a transition depending on the specifics of the simulation model and code – a modeling uncertainty. Considering all the orientation cases together, we observe a spread in the  $L_c$  values for the various types of damage that is greater than the spread for any given orientation. This spread constitutes an uncertainty band that depends on projectile orientation, convolved with the modeling uncertainty. By defining this wider band, we indicate an inherent uncertainty attached to any ballistic limit prediction that makes use of the SBM shape model. Thus, this uncertainty contributes to the damage uncertainty attachable to EVOLVE, and thence to the uncertainty in ORDEM2000.

Future work will extend the velocity range covered down to at least 7 km/s, and up to 15 km/s. Statistical methods will be applied to refine our statements about the uncertainty bands, and any variation of these bands with velocity.

## References

1. Williamsen, J. "Review of Space Shuttle Meteoroid/Orbital Debris Critical Risk Assessment Practices," IDA Paper P-3838, November 2003.
2. Reynold, R.C., et al. "NASA Standard Breakup Model, 1998 Revision." Lockheed Martin Space and Mission Systems and Services Report LMSMSS-32532, September 1998.
3. Evans, S., et al. "Comparison of SPHC Hydrocode Results with Penetration Equations and Results of Other Codes," AIAA 2004-1878, 45<sup>th</sup> SDM Conference, Palm Springs, CA, April 2004.
4. Hu, K., and Schonberg, W. P., "Ballistic Limit Curves for Non-Spherical Projectiles Impacting Dual-Wall Spacecraft Systems," Hypervelocity Impact Symposium, Noordwijk, Netherlands, December 2003.
5. Christiansen, E., and Kerr, J. "Ballistic Limit Equations for Spacecraft Shielding," *Int. J. Impact Engng.*, 2001; 26: 93-104.

Table 1: Flake impact aspect run matrix. Velocity 12 km/s, obliquity 1.6 deg.

"Edge-on" Cases			Lc (mm)	Mass (g)	Plastic Frac	Spall	Thru
Rx = 0 Ry = 0 Rz = 0	Rz = 0	4.0	4.0	0.039			
		4.5	4.5				
		5.0	5.0	0.071		X	
		5.5	5.5				
		6.0	6.0	0.115			X
	Rz = 45	4.0	4.0	0.039			
		4.5	4.5				
		5.0	5.0	0.071			
		5.5	5.5				
		6.0	6.0	0.115			
	Rz = 90	4.0	4.0	0.039	X		
		4.5	4.5				
		5.0	5.0	0.071			X
		5.5	5.5				
		6.0	6.0	0.115			X
"Corner-on" Cases							
Rx = 0 Ry = 45 Rz = 45	Rz = 45	4.0	4.0	0.039			
		4.5	4.5				
		5.0	5.0	0.071			
		5.5	5.5				
		6.0	6.0	0.115			
	Rz = 90	4.0	4.0	0.039			
		4.5	4.5				
		5.0	5.0	0.071			
		5.5	5.5				
		6.0	6.0	0.115			X
Sphere Cases							
	4.0	4.0	0.093		X		
	4.5	4.5					
	5.0	5.0					
	5.5	5.5					
	6.0	6.0	0.314			X	

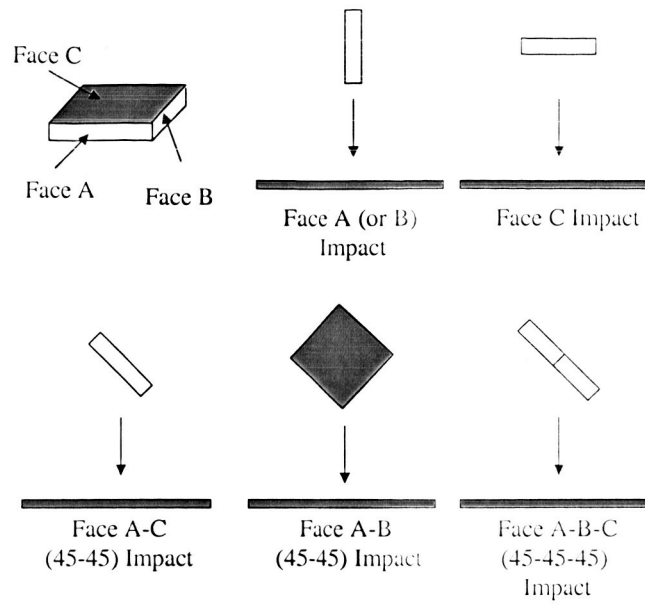


Figure 1: Impact flake geometry and impact orientations used in the simulations.

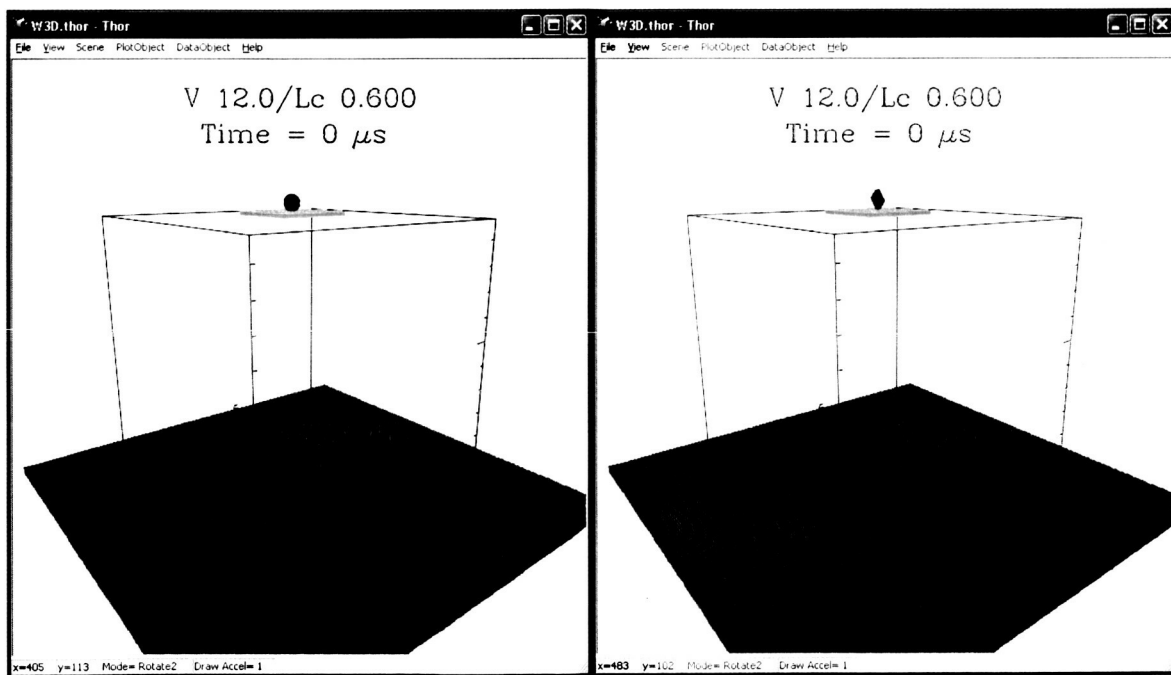


Figure 2: Sphere and flake setups, 3-D views.

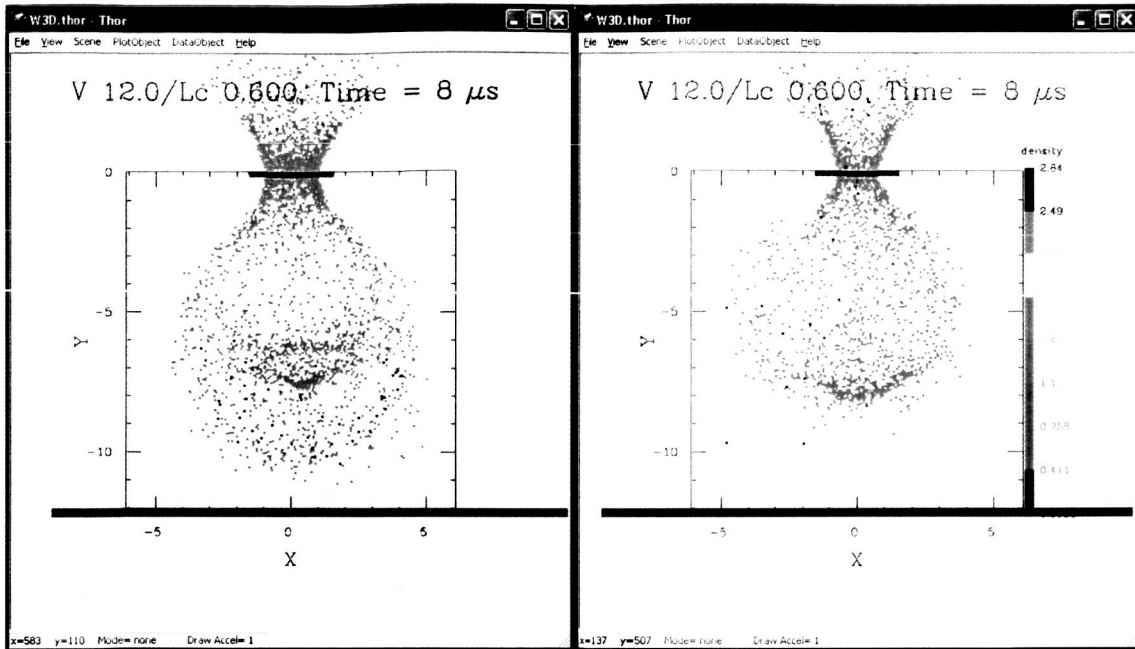


Figure 3: 2-D views of debris clouds of sphere (left) and flake (right).

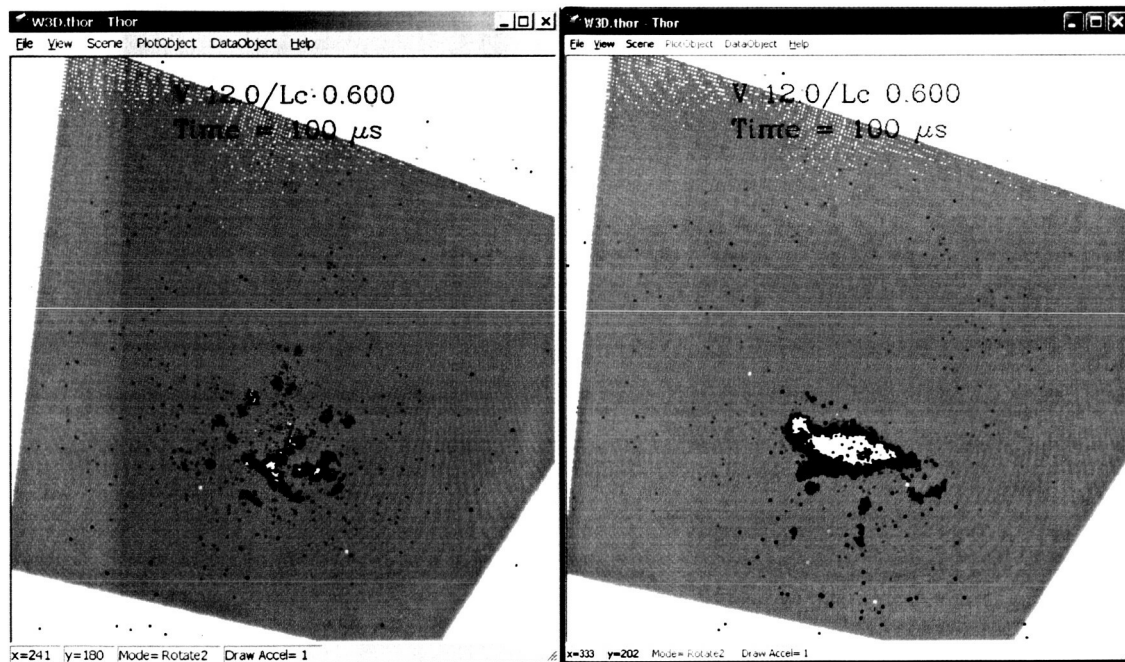


Figure 4: 3-D views of backwall damage by the sphere (left) and the flake (right); view is from behind the backwall. Dark blue material is fractured; light blue is plastically yielded; green is undisturbed solid. Through-holes are visible as white.